D.Kishore, Dr. T.Venkateswarlu / International Journal of Engineering Research and Applications (IJERA)
ISSN: 2248-9622 www.ijera.com
Vol. 2, Issue 3, May-Jun 2012, pp.139-146

Enhancement of Recognition Rate in Blurred Images Using Legendre Moment Invariants

D.Kishore*,Dr. T.Venkateswarlu**
*(Department of ECE, Sri Venkateswara University, Tirupati-517502)
**(Department of ECE, Sri Venkateswara University, Tirupati-517502)

Abstract
Processing blurred images is a key problem in many image applications. Existing methods to obtain blur invariants which are invariant with respect to centrally symmetric blur are based on geometric moments or complex moments. In this paper, we propose a new method to construct a set of blur invariants using the orthogonal Legendre moments. Some important proper-ties of Legendre moments for the blurred image are presented and proved. The performance of the proposed descriptors is evaluated with various point-spread functions and different image noises. The comparison of the present approach with previous methods in terms of pattern recognition accuracy is also provided. The experimental results show that the proposed descriptors are more robust to noise and have better discriminative power than the methods based on geometric or complex moments.

***Keywords*—Blur invariants, blurred image, Legendre moments, pattern recognition, symmetric blur.**

I. INTRODUCTION
IMAGE processing is a very active area that has impacts in many domains from remote sensing, robotics, traffic surveillance, to medicine. Automatic target recognition and tracking, character recognition, 3-D scene analysis and reconstruction are only a few objectives to deal with. Since the real sensing systems are usually imperfect and the environmental conditions are changing over time, the acquired images often provide a degraded version of the true scene. An important class of degradations we are faced with in practice is image blurring, which can be caused by diffraction, lens aberration, wrong focus, and atmospheric turbulence. In pattern recognition, two options have been widely explored either through a two steps approach by restoring the image and then applying recognition methods, or by designing a direct one-step solution, free of blurring effects. In the former case, the point spread function (PSF), most often unknown in real applications, should be estimated [1]–[5]. In the latter case, finding a set of invariants that are not affected by blurring is the key problem and the subject of this paper. The pioneering work in this field was performed by Flusser and Suk [6] who derived invariants to convolution with an arbitrary Centro-symmetric PSF. These invariants have been success-fully used in template matching of satellite images [6], in pat-tern recognition [7]–[10], in blurred digit and character recognition [11], [12], in normalizing blurred images into canonical forms [13], [14], and in focus/defocus quantitative measurement [15]. More recently, Flusser and Zitova introduced the combined blur-rotation invariants [16] and reported their successful application to satellite image registration [17] and camera motion estimation [18]. Suk and Flusser further proposed a set of combined invariants which are invariant to affine transform and to blur [19]. The extension of blur invariants to –dimensions has also been investigated [20], [21]. All the existing methods to derive the blur invariants are based on geometric moments or complex moments. However, both geometric moments and complex moments contain redundant information and are sensitive to noise especially when high-order moments are concerned. This is due to the fact that the kernel polynomials are not orthogonal. Teague has suggested the use of orthogonal moments to re-cover the image from moments [22]. It was shown that the orthogonal moments are better than other types of moments in terms of information redundancy, and are more robust to noise [23]. As noted by Teh and Chin [23], the moment invariants are considered reliable features in pattern recognition if they are in-sensitive to the presence of image noise. Consequently, it could be expected that the use of orthogonal moments in the construction of blur invariant provides better recognition results. To the authors' knowledge, no orthogonal moments have been used to construct the blur invariants. In this paper, we propose a new method to derive a set of blur invariants based on orthogonal Legendre moments (for a recent survey on moments, refer to [24]–[27]). The organization of this paper is as follows: in Section II, we review the theory of blur invariants of geometric moments and the definition of Legendre moments. In Section III, we establish a relationship between the Legendre moments of the blurred image and those of the original image and the PSF. Based on this relationship, a set of blur invariants using Legendre moments is provided. The experimental results for evaluating the performance of the proposed descriptors are given in Section IV. Finally, some concluding remarks are provided.

II. BLURINVARIANTS AND LEGENDRE MOMENTS

This section first reviews the theory of blur invariants of geometric moments proposed by Flusser and Suk [6], [7], and then presents some basic definitions of Legendre moments.

A. Blur Invariants of Geometric Moments

The 2-D geometric moment of order $(P+Q)$, with image intensity function $f(x,y)$, is defined as

$$m_{pq}^{(f)} = \int_{-1}^{1}\int_{-1}^{1} x^p y^q f(x,y)\,dxdy$$

where, without loss of generality, we assume that the image function $f(x,y)$ is defined on the square $[-1,1]X[-1,1]$. The corresponding central moment of image $f(x,y)$ is de-fined as

$$\mu_{pq}^{(f)} = \int_{-1}^{1}\int_{-1}^{1} (x-x_0^{(f)})^p (y-y_0^{(f)})^q f(x,y)\,dxdy$$

with the coordinates denoting $(x_o^{(f)} y_o^{(f)})$ the centroid of $f(x,y)$

$$x_0^{(f)} = \frac{m_{10}^{(f)}}{m_{00}^{(f)}}, \quad y_0^{(f)} = \frac{m_{01}^{(f)}}{m_{00}^{(f)}}.$$

Let $g(x,y)$ be a blurred version of the original image $f(x,y)$. The blurring is classically described by the convolution

$$g(x,y) = (f * h)(x,y)$$

where h(x,y) is the PSF of the imaging system, and * denotes linear convolution. In this paper, we assume that the PSF, $h(x,y)$, is a centrally symmetric image function and the imaging system is energy-preserving, that is,

$$h(x,y) = h(-x,-y)$$
$$\int_{-1}^{1}\int_{-1}^{1} h(x,y)\,dxdy = 1.$$

As noted by Flusser [7], the assumption of centrally symmetry is not a significant limitation of practical utilization of the method. Most real sensors and imaging systems have PSFs with certain degrees of symmetry. In many cases they have even higher symmetry than central, such as axial or radial symmetry. Thus, the central symmetry assumption is general enough to describe almost all practical situations.

Lemma 1: The centroid of the blurred image $g(x,y)$ is related to the centroid of the original image $f(x,y)$ and that of the PSF $h(x,y)$ as

$$x_0^{(g)} = x_0^{(f)} + x_0^{(h)}$$
$$y_0^{(g)} = y_0^{(f)} + y_0^{(h)}.$$

In particular, if $h(x,y)$ is centrally symmetric, then $x_o^{(h)} = y_o^{(h)} = 0$. In such a case, we have $, x_o^{(g)} = x_o^{(f)}, y_o^{(g)} = y_o^{(f)}$. The proof of Lemma 1 can be found in [9].

B. Legendre Moments

The 2-D $(p+q)$th order Legendre moment of image function $f(x,y)$ is defined as [28]

$$L_{pq}^{(f)} = \int_{-1}^{1}\int_{-1}^{1} P_p(x) P_q(y) f(x,y)\,dxdy$$

where $P_p(x)$ is the p^{th}-order orthonormal Legendre polynomials given by

$$P_p(x) = \sum_{k=0}^{p} c_{p,k} x^k$$

With

$$c_{p,k} = \begin{cases} \sqrt{\frac{2p+1}{2}} \frac{(-1)^{\frac{p-k}{2}}(p+k)!}{2^p \left(\frac{p-k}{2}\right)!\left(\frac{p+k}{2}\right)!k!}, & p-k = \text{even} \\ 0, & p-k = \text{odd}. \end{cases}$$

The corresponding central moments are defined as

$$\bar{L}_{pq}^{(f)} = \int_{-1}^{1}\int_{-1}^{1} P_p(x-x_0^{(f)}) P_q(y-y_0^{(f)}) f(x,y)\,dxdy$$

III. METHOD

In this section, we first establish a relationship between the Legendre moments of the blurred image and those of the original image and the PSF. We then derive a set of blur moment invariants.

A. Legendre Moments of the Blurred Image

The 2-D normalized Legendre moments of blurred image, $f(x,y)$ are

$$\begin{aligned} L_{p,q}^{(g)} &= \int_{-1}^{1}\int_{-1}^{1} P_p(x) P_q(y) g(x,y)\,dxdy \\ &= \int_{-1}^{1}\int_{-1}^{1} P_p(x) P_q(y) (f*h)(x,y)\,dxdy \\ &= \int_{-1}^{1}\int_{-1}^{1} P_p(x) P_q(y) \left(\int_{-\infty}^{\infty}\int_{-\infty}^{\infty} h(a,b) f(x-a,y-b)\,dadb\right) dxdy \\ &= \int_{-1}^{1}\int_{-1}^{1} h(a,b) \left(\int_{-1}^{1}\int_{-1}^{1} P_p(x+a) P_q(y+b) f(x,y)\,dxdy\right) dadb \end{aligned}$$

In the rest of this subsection, we discuss how to express the Legendre moments of blurred image in terms of Legendre moments of the original image and the PSF.

Making the notation $U_M(x) = (P_0(x), P_1(x), \ldots \ldots P_M(x))^T$ and $M_M(x) = (1, x, \ldots x^M)^T$ where the superscript T indicates the vector transposition, we have

$$U_M(x) = C_M M_M(x)$$

where $C_M = (C_p, k)$, with $0 \le k \le p \le M$, is $(M+1)X(M+1)$ a lower triangular matrix.

Since all the diagonal elements of $C_M, C_{p,p} = \sqrt{2p + \frac{1}{2}}(2p)!/2^p p!$, are not zero, the matrix C_M is nonsingular, thus

$$M_M(x) = (C_M)^{-1} U_M(x) = D_M U_M(x)$$

where $D_M = (d_p, k)$, with $0 \le k \le p \le M$, is the inverse matrix of C_M.

$$d_{p,k} = \begin{cases} \sqrt{\frac{2}{2k+1}} \dfrac{2^{3k-p/2}}{\left(\frac{p-k}{2}\right)! \prod_{j=1}^{(p-k)/2} (2k+2j+1)} \dfrac{p!k!}{(2k)!}, & p-k = \text{even} \\ 0, & p-k = \text{odd}. \end{cases}$$

By expanding, we obtain

$$x^k = \sum_{i=0}^{k} d_{k,i} P_i(x).$$

Similarly

$$a^m = \sum_{s=0}^{m} d_{m,s} P_s(a).$$

Replacing the variable x by x+a, we have

$$P_p(x+a) = \sum_{m=0}^{p} c_{p,m}(x+a)^m = \sum_{m=0}^{p}\sum_{k=0}^{m} \binom{m}{k} c_{p,m} x^k a^{m-k}.$$

Substituting these values we will get,

$$\begin{aligned} P_p(x+a) &= \sum_{m=0}^{p}\sum_{k=0}^{m} \binom{m}{k} c_{p,m} \\ &\quad \times \sum_{i=0}^{k} d_{k,i} P_i(x) \sum_{s=0}^{m-k} d_{m-k,s} P_s(a) \\ &= \sum_{m=0}^{p}\sum_{k=0}^{m}\sum_{i=0}^{k}\sum_{s=0}^{m-k} \binom{m}{k} \\ &\quad \times c_{p,m} d_{k,i} d_{m-k,s} P_i(x) P_s(a) \\ &= \sum_{i=0}^{p}\sum_{k=i}^{p}\sum_{m=k}^{p}\sum_{s=0}^{m-k} \binom{m}{k} \\ &\quad \times c_{p,m} d_{k,i} d_{m-k,s} P_i(x) P_s(a). \end{aligned}$$

Similarly we have,

$$P_q(y+b) = \sum_{j=0}^{q}\sum_{l=j}^{q}\sum_{n=l}^{q}\sum_{t=0}^{n-l} \binom{n}{l} c_{q,n} d_{l,j} d_{n-l,t} P_j(y) P_t(b).$$

The following theorem reveals the relationship between the Legendre moments of the blurred image and those of the original image and the PSF.

Theorem 1: Let $f(x,y)$ be the original image function and the PSF $h(x,y)$ be an arbitrary image function, and $g(x,y)$ be a blurred version of $f(x,y)$, then the relations

$$\begin{aligned} L_{p,q}^{(g)} &= \sum_{i=0}^{p}\sum_{j=0}^{q} L_{i,j}^{(f)} \sum_{s=0}^{p-i}\sum_{t=0}^{q-j} L_{s,t}^{(h)} \sum_{k=i}^{p-s}\sum_{m=k+s}^{p}\sum_{l=j}^{q-t} \\ &\quad \times \sum_{n=l+t}^{q} \binom{m}{k}\binom{n}{l} c_{p,m} c_{q,n} d_{k,i} d_{m-k,s} d_{l,j} d_{n-l,t}, \end{aligned}$$

And

$$\begin{aligned} \bar{L}_{p,q}^{(g)} &= \sum_{i=0}^{p}\sum_{j=0}^{q} \bar{L}_{i,j}^{(f)} \sum_{s=0}^{p-i}\sum_{t=0}^{q-j} \bar{L}_{s,t}^{(h)} \sum_{k=i}^{p-s}\sum_{m=k+s}^{p}\sum_{l=j}^{q-t}\sum_{n=l+t}^{q} \\ &\quad \times \binom{m}{k}\binom{n}{l} c_{p,m} c_{q,n} d_{k,i} d_{m-k,s} d_{l,j} d_{n-l,t} \end{aligned}$$

hold for every p and q.

Proof: substituting the values we have,

$$\begin{aligned} L_{p,q}^{(g)} &= \int_{-1}^{1}\int_{-1}^{1} h(a,b) \left(\int_{-1}^{1}\int_{-1}^{1} \left(\sum_{i=0}^{p}\sum_{k=i}^{p}\sum_{m=k}^{p}\sum_{s=0}^{m-k} \binom{m}{k} c_{p,m} d_{k,i} d_{m-k,s} P_i(x) P_s(a) \right) \right. \\ &\quad \left. \times \left(\sum_{j=0}^{q}\sum_{l=j}^{q}\sum_{n=l}^{q}\sum_{t=0}^{n-l} \binom{n}{l} c_{q,n} d_{l,j} d_{n-l,t} P_j(y) P_t(b) \right) f(x,y)\,dx\,dy \right) da\,db. \end{aligned}$$

It can be rewritten as

$$\begin{aligned} L_{p,q}^{(g)} &= \sum_{i=0}^{p}\sum_{k=i}^{p}\sum_{m=k}^{p}\sum_{s=0}^{m-k}\sum_{j=0}^{q}\sum_{l=j}^{q}\sum_{n=l}^{q}\sum_{t=0}^{n-l} \binom{m}{k}\binom{n}{l} \\ &\quad \times c_{p,m} d_{m-k,s} d_{k,i} c_{q,n} d_{n-l,t} d_{l,j} L_{i,j}^{f} L_{s,t}^{h} \\ &= \sum_{i=0}^{p}\sum_{j=0}^{q} L_{i,j}^{(f)} \sum_{s=0}^{p-i}\sum_{t=0}^{q-j} L_{s,t}^{(h)} \sum_{k=i}^{p-s}\sum_{m=k+s}^{p}\sum_{l=j}^{q-t}\sum_{n=l+t}^{q} \\ &\quad \times \binom{m}{k}\binom{n}{l} c_{p,m} c_{q,n} d_{k,i} d_{m-k,s} d_{l,j} d_{n-l,t}. \end{aligned}$$

Theorem 2: If $f(x,y)$ satisfies the conditions of central symmetry, then

(a) $L_{p,q}^{(h)} = \bar{L}_{p,q}^{(h)}$ for every p and q;

(b) If $(p+q)$ is odd, then $\bar{L}_{p,q}^{(h)} = 0$.

B. Blur Invariants of Legendre Moments

With the help of Theorems 1 and 2, we are now ready to construct a set of blur invariants of Legendre moments through the following theorem.

Theorem 3: Let $f(x,y)$ be an image function. Let us define the following function $I^{(f)}: NXN \rightarrow R$.

If $(p+q)$ is even then

$$I(p,q)^{(f)} = 0.$$

If $(p+q)$ is odd, then

$$\begin{aligned} I(p,q)^{(f)} &= L_{p,q}^{(f)} - \frac{1}{2L_{0,0}^{(f)}} \sum_{i=0}^{p} \sum_{\substack{j=0 \\ 0<i+j<p+q}}^{q} \\ &\times I(i,j)^{(f)} \sum_{s=0}^{p-i} \sum_{t=0}^{q-j} L_{s,t}^{(f)} \sum_{k=i}^{p-s} \sum_{m=k+s}^{p} \sum_{l=j}^{q-t} \\ &\times \sum_{n=l+t}^{q} \binom{m}{k} \binom{n}{l} c_{p,m} c_{q,n} d_{k,i} d_{m-k,s} d_{l,j} d_{n-l,t}. \end{aligned}$$

Then, $I(p,q)$ is invariant to centrally symmetric blur for any p and q. The number $p+q$ is called the order of the invariant.

Theorem 4: Let $f(x,y)$ be an image function. Let us define the following function $\bar{I}^{(f)}: NXN \rightarrow R$.

If $(p+q)$ is even then $\bar{I}(p,q)^{(f)} = 0$

Fig. 1. Standard gray-level image of cat with size 128x 128.

If $(p+q)$ is odd then

$$\begin{aligned} \bar{I}(p,q)^{(f)} &= \bar{L}_{p,q}^{(f)} - \frac{1}{2\bar{L}_{0,0}^{(f)}} \sum_{i=0}^{p} \sum_{\substack{j=0 \\ 0<i+j<p+q}}^{q} \\ &\times \bar{I}(i,j)^{(f)} \sum_{s=0}^{p-i} \sum_{t=0}^{q-j} \bar{L}_{s,t}^{(f)} \sum_{k=i}^{p-s} \sum_{m=k+s}^{p} \sum_{l=j}^{q-t} \\ &\times \sum_{n=l+t}^{q} \binom{m}{k} \binom{n}{l} c_{p,m} c_{q,n} \\ &\times d_{k,i} d_{m-k,s} d_{l,j} d_{n-l,t}. \end{aligned}$$

Then, $\bar{I}(p,q)$ is invariant to centrally symmetric blur and to translation for any p and q.

IV. E XPERIMENTAL RESULTS

In this section, some experiments are described in order to show the invariance of the proposed method to various PSF's and its robustness to different kinds of noise. The comparison with some existing methods in terms of recognition accuracy is also provided.

A. Test of Invariance and Robustness to Noise

A toy cat image, whose size is 128x 128 (Fig. 1), has been chosen from the public Columbia database [30]. This image was then successively degraded by out-of-focus blur, averaging mask, Gaussian function and motion filter as reported in [8], [9], and [19]. The parameter σ(standard deviation of the Gaussian function) of Gaussian blur was chosen equal to 0.5, and the parameter θ (θ means the angle in the counterclockwise direction, $\theta = 0$ corresponds to a horizontal motion, and $\theta = \frac{\pi}{2}$ corresponds to a vertical motion) of motion blur set to 0.

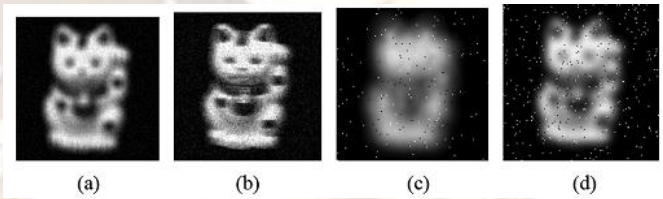

Fig. 2. Some examples of the blurred image: (a) averaging blur with additive zero-mean Gaussian noise, STD=10; (b) motion blur with additive zero-mean Gaussian noise, STD=20; (c) out-of-focus blur with additive salt-and-pepper noise, density =0.01 (d) Gaussian blur with additive salt-and-pepper noise, density = 0.02.

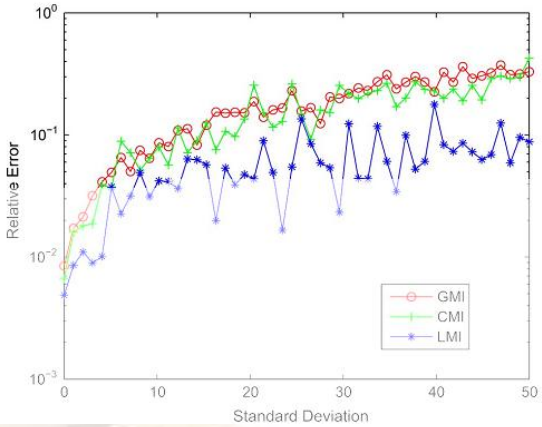

Fig. 3. Relative error for averaging blur with Gaussian noise shown in Fig. 2(a). Horizontal axis: standard deviation of noise; vertical axis: relative error between the corrupted image and original image.

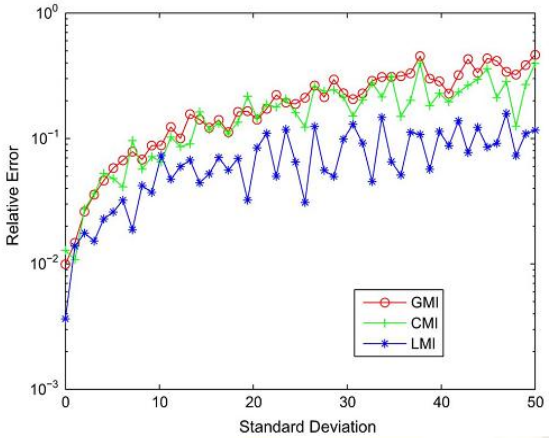

Fig. 4. Relative error for motion blur with Gaussian noise shown in Fig. 2(b). Horizontal axis: standard deviation of noise; vertical axis: relative error between the corrupted image and original image.

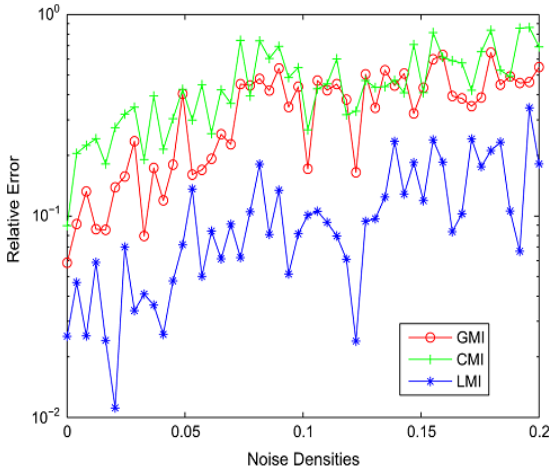

Fig. 5. Relative error for out-of-focus blur with salt-and-pepper noise shown in Fig. 2(c). Horizontal axis: noise density; vertical axis: relative error between the corrupted image and original image.

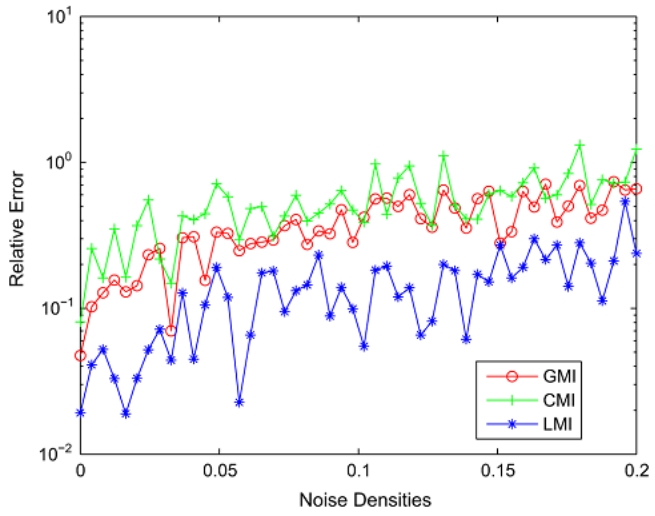

Fig. 6. Relative error for Gaussian blur adding salt-and-pepper noise shown in Fig. 2(d). Horizontal axis: noise density; vertical axis: relative error between the corrupted image and original image.

Other parameters such as the size for averaging blur, the radius for out-of-focus and the depth for motion filter were chosen equal to the size of blur mask in all the experiments. We first checked that the eighteen Legendre moment invariants of order up to seven were exactly equal to those of the original image whatever the blurring mode.

Let us define the vectors $\tilde{I}_r = (I(0,r), I(1,r-1), \ldots\ldots\ldots, I(r,0))$ and $I(r) = (I_3, I_5, I_7, \ldots\ldots I_r$ for any odd value of $r \geq 3$. The relative error between the two images is computed by

$$E_r(f,g) = \frac{\left\| \tilde{I}^{(f)}(r) - \tilde{I}^{(g)}(r) \right\|}{\left\| \tilde{I}^{(f)}(r) \right\|}$$

where ||.|| is Euclidean norm in L^2 space. In the following experiments, moment invariants of order up to r=7 are used.

The next experiment was carried out to verify the performance of the invariants to both image blur and noise. The original cat image was blurred by a 9x 9 averaging mask and a zero-mean Gaussian noise with standard deviation (STD) from 1 to 50 was added. Some examples of the blurred image with additive Gaussian noise or salt-and-pepper noise are shown in Fig. 2. Plots in Fig. 3 compare the relative error defined by (27) for Flusser's method based on geometric moment invariants (GMI)

Fig. 7. Original images of alphanumeric characters for invariant character recognition.

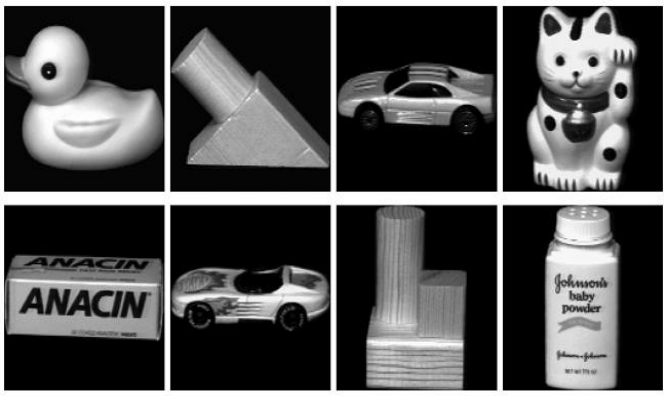

Fig. 8. Eight objects selected from the Coil-100 image database of Columbia University.

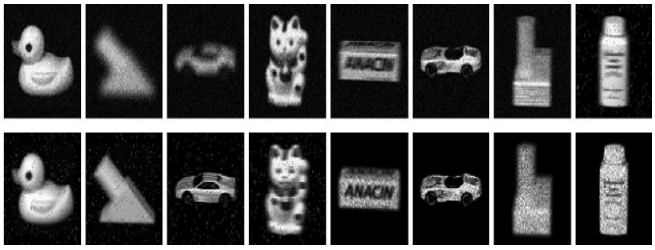

Fig. 9. Some examples of the blurred images corrupted by various types of noise

TABLE I
RECOGNITION RATES OBTAINED RESPECTIVELY WITH GMI, CMI AND LMI FOR ALPHANUMERIC CHARACTER IN FIG. 7

	GMI	CMI	LMI
Noise-free	100%	100%	100%
Additive white noise with STD=1	92.08%	91.88%	100%
Additive white noise with STD=3	85%	82.92%	97.71%
Additive white noise with STD=5	77.29%	75.42%	90%
Additive salt-and-pepper noise with noise density = 0.2%	91.04%	87.08%	97.92%
Additive salt-and-pepper noise with noise density = 0.4%	83.75%	83.54%	94.79%
Additive salt-and-pepper noise with noise density = 0.8%	77.33%	75.67%	90%
Additive multiplicative noise with noise density = 0.01	95.83%	90.63%	98.13%
Additive multiplicative noise with noise density = 0.03	95%	86.88%	97.5%
Additive multiplicative noise with noise density = 0.05	91.25%	85.21%	95%
Computation time	6.86s	27.08s	6.95s

where eighteen blur invariants derived from central moments are used [7], the complex moment invariants (CMI) reported in [16] and the present Legendre moment invariants (LMI) up to order seven by averaging blur with different Gaussian noises. It can be seen from the figure that the proposed descriptors per-form better than the GMI and CMI. Then, the cat image was

TABLE II
RECOGNITION RATES OF THE GMI, CMI AND LMI IN OBJECT RECOGNITION (FIG. 9)

	GMI	CMI	LMI
Noise-free	100%	100%	100%
Additive white noise with STD=8	78.33%	80%	96.25%
Additive white noise with STD=16	68.96%	62.71%	83.96%
Additive white noise with STD=25	60.42%	50.62%	74.79%
Additive salt-and-pepper noise with noise density = 0.01	87.29%	76.46%	97.08%
Additive salt-and-pepper noise with noise density = 0.02	73.33%	64.38%	85.83%
Additive salt-and-pepper noise with noise density = 0.03	68.13%	56.46%	79.37%
Additive multiplicative noise with noise density = 0.1	100%	99.17%	100%
Additive multiplicative noise with noise density = 0.3	96.25%	87.92%	99.38%
Additive multiplicative noise with noise density = 0.5	90%	81.88%	95.63%
Computation time	9.42s	44.14s	9.80s

blurred by a 11x 11 motion filter, and the same Gaussian noise was added. The results (Fig. 4) again indicate the better behavior of the proposed method. Similarly, the original cat image was degraded on one hand by out-of-focus blur (13 pixel-radius of the PSF support) and by adding a salt-and-pepper noise with noise densities varying from 0.004 to 0.2 (see Fig. 5) and, on another hand, by Gaussian blur (the PSF was a Gaussian function with 15 pixel-radius of support) with the same salt-and-pepper noise (see Fig. 6). It can be also seen that a better robustness is achieved whatever the PSF or the additive noises.

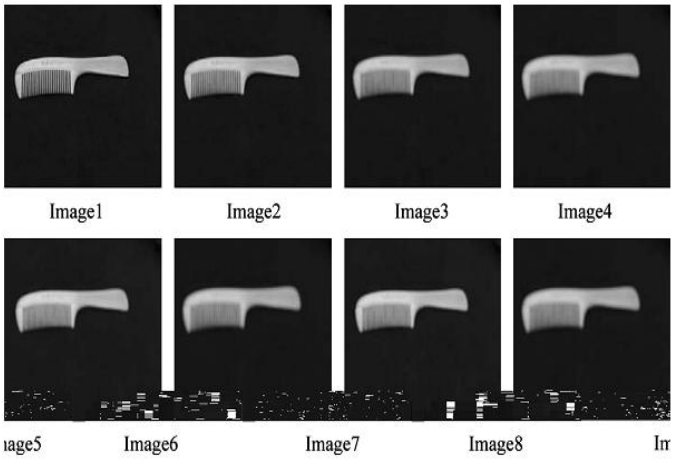

Fig. 10. The comb. The extent of out-of-focus blur increases from Image1 to Image8.

B. Classification Results

This experiment was carried out to compare the discrimination power of the GMI, CMI and LMI. A set of alphanumeric characters whose size is 50x 50 pixels (Fig. 7) is used for the recognition task. The reason for choosing such a character set is that the elements in subset {0, o}, {2, Z}, {7, T}, and {9, q} can be easily misclassified due to their similarity. The testing set is generated by adding averaging blur, out-of-focus blur, Gaussian blur and motion blur with mask of sizes 3x 3, 4x 4, 5x 5, 6x 6, 7x 7, 8x 8, 9x 9, 10x10, 11x 11, 12x12 pixels, respectively. The parameter of Gaussian blur was chosen equal to 1 or 2, and the parameter of motion blur set to 0 or 1, forming a set of 480 images. Note that the original images as well as the blurred images are mapped onto the area of orthogonality, and the actual size of the blurred images in this experiment is 80x 80. This is followed by adding a white Gaussian noise with different standard deviations, salt-and-pepper noise with different noise densities and multiplicative noise with different noise densities. The Euclidean distance is used here as the classification measure. Table I shows the classification rates using the different moment invariants. One can observe from this table that the recognition results are quite good for the different methods in the noise-free case. The classification rates remain high for low and moderate noise levels but decrease significantly when the noise level goes up. However, if the GMI behaves better than the CMI, the LMI approach is the only one providing a rate close to or

over 90% whatever the noise nature and its level. In the next example, eight objects were selected from the Coil-100 image database of Columbia University as an original image set (see Fig. 8). The actual size of the blurred images in this experiment is 160x 160. Fig. 9 shows some examples of the blurred and corrupted images. The recognition results are displayed in Table II. They lead to the same conclusions regarding the performance of the respective moment invariants but the decrease in recognition rate is more significant when the noise level is increased. This is also true for the LMI. The CMI do not perform well in these experiments due to their additional invariance to rotation. The worse numerical stability is a tax on the combined invariance. The orthogonality of LMI explains the difference in performance with GMI. We also compared the computational load of the GMI, CMI and LMI in these two experiments. The programs were implemented in MATLAB 6.5 on a PC P4 2.4 GHZ, 512M RAM. It can be seen from Tables I and II that the GMI and the LMI computations are much faster than the CMI ones. This is due to the fact that the computation of the complex moments requires a mapping transformation which is time consuming.

C. Real Image Analysis

In the last experiment, we tested the performance of the invariants on images degraded by real out-of-focus blur. A sequence of eight pictures of a comb lying on a black ground was taken by a digital camera (Panasonic DMC-FZ50). The images differ from each other by the level of out-of-focus blur. The picture was captured 8 times from the same position but with different focus depth, manually set. All the test images are depicted in Fig. 10. The values of GMI, CMI, and LMI were computed for each image. Table III depicts the values of $\frac{\sigma}{\mu}$, where μ denotes the mean of eight real images and σ the standard deviation. From this table, it can be seen that the minimal value of the LMI is 3.42% and the maximum value of the LMI is 6.15%, which are lower than those obtained with GMI (resp. 4.91%, 12.43%) and the CMI (resp. 7.47%, 7.54%).

TABLE III
GMI CMI AND LMI VALUES OF THE REAL IMAGES IN FIG. 10

	Image1	Image2	Image3	Image4	Image5	Image6	Image7	Image8	σ/μ
$\bar{G}(5,0)$	-0.328	-0.319	-0.324	-0.322	-0.324	-0.329	-0.357	-0.363	5.07%
$\bar{C}(5,0)$	35.01	34.95	34.51	34.34	34.38	34.44	40.28	40.62	7.54%
$\bar{L}(5,0)$	-66.3	-66.3	-68.2	-68.5	-69.1	-69.9	-71.9	-72.8	3.42%
$\bar{G}(4,1)$	-0.0622	-0.0658	-0.0671	-0.0669	-0.0669	-0.0674	-0.0720	-0.0725	4.91%
$\bar{C}(4,1)$	50.20	50.02	49.40	49.18	49.21	49.33	57.61	58.15	7.5%
$\bar{L}(4,1)$	-11.4	-12.4	-12.8	-12.9	-13.0	-13.0	-13.1	-13.2	4.62%
$\bar{G}(3,2)$	-0.0190	-0.0179	-0.0174	-0.0165	-0.0166	-0.0169	-0.0219	-0.0222	12.43%
$\bar{C}(3,2)$	60.14	59.86	59.13	58.88	58.90	59.07	68.92	69.59	7.47%
$\bar{L}(3,2)$	-12.9	-13.0	-13.4	-13.4	-13.5	-13.7	-14.2	-14.3	3.72%
$\bar{G}(2,3)$	-0.0262	-0.0278	-0.0278	-0.0274	-0.0273	-0.0274	-0.0313	-0.0316	6.98%
$\bar{C}(2,3)$	60.14	59.86	59.13	58.88	58.90	59.07	68.92	69.59	7.47%
$\bar{L}(2,3)$	-10.6	-11.7	-12.1	-12.2	-12.2	-12.2	-12.5	-12.5	5.16%
$\bar{G}(1,4)$	-0.0485	-0.0479	-0.0480	-0.0468	-0.0471	-0.0475	-0.0549	-0.0554	7.11%
$\bar{C}(1,4)$	50.20	50.02	49.40	49.18	49.21	49.33	57.61	58.15	7.5%
$\bar{L}(1,4)$	-8.84	-8.79	-8.89	-8.72	-8.79	-8.86	-9.98	-10.06	6.15%
$\bar{G}(0,5)$	-0.223	-0.250	-0.257	-0.257	-0.257	-0.258	-0.269	-0.269	5.67%
$\bar{C}(0,5)$	35.01	34.95	34.51	34.34	34.38	34.44	40.28	40.62	7.54%
$\bar{L}(0,5)$	-40.6	-45.4	-46.8	-46.8	-46.9	-47.1	-48.6	-48.6	5.49%

V. CONCLUSION ANDPERSPECTIVES

In this paper, we have proposed a new approach to derive a 1set of blur invariants using the orthogonal Legendre moments. The relationship between the Legendre moments of the blurred image and those of the original image and the PSF has been established, and using this relationship, a set of blur invariants based on Legendre moments has been derived. The experiments conducted so far in very distinct situations demonstrated that the proposed descriptors are more robust to noise and have better discriminative power than the methods based on geometric or complex moments.

One weak point of these descriptors is that they are only invariant to translation, but not invariant under image scaling and rotation. The derivation of combined invariants to both geometric transformation and blur is currently under investigation.

ACKNOWLEDGMENT

The authors would like to thank the reviewers and Associate Editor Dr. Kuruoglu for their insightful suggestions which helped improve the manuscript.

REFERENCES

[1] P. Campisi and K. Egiazarian, Blind Image Deconvolution: Theory and Applications. Boca Raton, FL: CRC, 2007.

[2] A. Savakis and H. J. Trussell, "Blur identification by residual spectral matching,"IEEE. Trans. Image Process. , vol. 2, no. 2, pp. 141–151, Feb. 1993.

[3] R. Molina, J. Mateos, and A. K. Katsaggelos, "Blind deconvolution using a variational approach to parameter, image, and blur estimation," IEEE Trans. Image Process., vol. 15, no. 12, pp. 3715–3727, Dec. 2006.

[4] M. Sorel and J. Flusser, "Space-variant restoration of images degraded by camera motion blur," IEEE Trans. Image Process. , vol. 17, no. 2, pp. 105–116, Feb. 2008.

[5] S. W. Jung, T. H. Kim, and S. J. Ko, "A novel multiple image deblur-ring technique using fuzzy projection onto convex sets," IEEE Signal Process. Lett., vol. 16, no. 3, pp. 192–195, Mar. 2009.

[6] J. Flusser, T. Suk, and S. Saic, "Recognition of blurred images by the method of moments," IEEE Trans. Image Process. , vol. 5, no. 3, pp. 533–538, Mar. 1996.

[7] J. Flusser and T. Suk, "Degraded image analysis: An invariant ap-proach," IEEE Trans. Pattern Anal. Mach. Intell. , vol. 20, no. 6, pp. 590–603, Jun. 1998.

[8] J. Liu and T. X. Zhang, "Recognition of the blurred image by com-plex moment invariants," Pattern Recognit. Lett., vol. 26, no. 8, pp. 1128–1138, 2005.

[9] J. Flusser, T. Suk, and S. Saic, "Recognition of images degraded by linear motion blur without restoration," Comput. Suppl., vol. 11, pp. 37–51, 1996.

[10] A. Stern, I. Kruchakov, E. Yoavi, and S. Kopeika, "Recognition of mo-tion-blurred images by use of the method of moments," Appl. Opt., vol. 41, no. 11, pp. 2164–2172, 2002.

[11] J. Lu and Y. Yoshida, "Blurred image recognition based on phase in-variants," IEICE Trans. Fundam. Electron. Comm. Comput. Sci. , vol. E82A, pp. 1450–1455, 1999.

[12] X. H. Wang and R. C. Zhao, "Pattern recognition by combined invari-ants," Chin. J. Electron., vol. 10, no. 4, pp. 480–483, 2001. [13] Y. Zhang, C. Wen, and Y. Zhang, "Estimation of motion parameters from blurred images," Pattern Recognit. Lett., vol. 21, no. 5, pp. 425–433, 2000.

[14] Y. Zhang, C. Wen, Y. Zhang, and Y. C. Soh, "Determination of blur and affine combined invariants by normalization," Pattern Recognit., vol. 35, no. 1, pp. 211–221, 2002.

[15] Y. Zhang, Y. Zhang, and C. Wen, "A new focus measure method using moments,"Image Vis. Comput., vol. 18, no. 12, pp. 959–965, Dec. 2000.

[16] J. Flusser and B. Zitova, "Combined invariants to linear filtering and rotation," Int. J. Pattern Recognit. Artif. Intell. , vol. 13, no. 8, pp. 1123–1136, 1999.

[17] J. Flusser, B. Zitova, and T. Suk, I. Tammy, Ed., "Invariant-based registration of rotated and blurred images," in Proc. IEEE Int. Geo-science and Remote Sensing Symp. , Hamburg, Germany, Jun. 1999, pp. 1262–1264.

[18] B. Zitova and J. Flusser, "Estimation of camera planar motion from defocused images," in Proc. IEEE Int. Conf. Image Processing , Rochester, NY, Sep. 2002, vol. II, pp. 329–332.

[19] T. Suk and J. Flusser, "Combined blur and affine moment invariants and their use in pattern recognition," Pattern Recognit. , vol. 36, no. 12, pp. 2895–2907, 2003.

[20] J. Flusser, J. Boldys, and B. Zitova, "Moment forms invariant to rota-tion and blur in arbitrary number of dimensions," IEEE Trans. Pattern Anal. Mach. Intell., vol. 25, no. 2, pp. 234–246, Feb. 2003.

[21] F. M. Candocia, "Moment relations and blur invariant conditions for finite-extent signals in one, two and N-dimensions," Pattern Recognit. Lett. , vol. 25, no. 4, pp. 437–447, 2004.

[22] M. Teague, "Image analysis via the general theory of moments," J. Opt. Soc. Amer., vol. 70, no. 8, pp. 920–930, 1980.

[23] C. H. Teh and R. T. Chin, "On image analysis by the method of mo-ments,"IEEE Trans. Pattern Anal. Mach. Intell. , vol. 10, no. 4, pp. 496–513, Apr. 1988.

[24] H. Z. Shu, L. M. Luo, and J. L. Coatrieux, "Moment-based approaches in image Part 1: Basic features," IEEE Eng. Med. Biol. Mag., vol. 26, no. 5, pp. 70–75, 2007.

[25] H. Z. Shu, L. M. Luo, and J. L. Coatrieux, "Moment-based approaches in image Part 2: Invariance," IEEE Eng. Med. Biol. Mag., vol. 27, no. 1, pp. 81–83, 2008.

[26] H. Z. Shu, L. M. Luo, and J. L. Coatrieux, "Moment-based approaches in image Part 3: Computational considerations," IEEE Eng. Med. Biol. Mag., vol. 27, no. 3, pp. 89–91, 2008.

[27] H. Z. Shu, L. M. Luo, and J. L. Coatrieux, "Moment-based approaches in imaging Part 4: Some applications,"IEEE Eng. Med. Biol. Mag. , vol. 27, no. 5, pp. 116–118, May 2008.

[28] R. Mukundan and K. R. Ramakrishnan, Moment Functions in Image Analysis-Theory and Applications. Singapore: World Scientific, 1998.

[29] H. Z. Shu, J. Zhou, G. N. Han, L. M. Luo, and J. L. Coatrieux, "Image reconstruction from limited range projections using orthogonal mo-ments,"Pattern Recognit. , vol. 40, no. 2, pp. 670– 680, 2007.

[30] [Online]. Available: http://www1.cs.columbia.edu/CAVE/soft-ware/softlib/coil-20.php